



JOINT INSTITUTE FOR NUCLEAR RESEARCH
Frank Laboratory of Neutron Physics

FINAL REPORT ON THE SUMMER STUDENT PROGRAM

*Small-angle X-ray scattering of alginate
membranes doped with CoFe_2O_4
nanoparticles*

Supervisor:

Dr. Bălăsoiu Maria

Student:

Pahomi Alexandru, Romania
West University of Timișoara

Participation period:

July 15 – August 25

Dubna, 2018

Abstract

Today, alginate is one of the most employed biopolymers in agricultural, food and life science related industry, mostly due to its high performance gelling and viscosity properties. The initial industrial uses of alginates were as adhesive binders, however more recently they are extensively used as thickeners, emulsifiers, film and gels making substances. The complementary use of alginate and magnetic nanoparticles can lead to new biomedical and biotechnological applications, including targeted drug delivery, magnetic cell separation, enzyme immobilization, magnetic resonance imaging (MRI), and hyperthermia treatments.

In this study are presented the structural investigations of alginate membranes doped with CoFe_2O_4 nanoparticles and the effect of their cross-linking with CaCl_2 using atomic force microscopy (AFM), scanning electron microscopy (SEM), X-ray diffraction (XRD) and small-angle X-ray scattering (SAXS).

Content

Introduction	3
Experimental section	4
Materials and membrane preparation	4
Methods of characterization	4
Small-angle X-ray scattering (SAXS)	4
Atomic Force Microscopy (AFM)	5
Scanning Electron Microscopy (SEM).....	6
X-ray Diffraction (XRD)	6
Results and Discussion	7
Surface morphology	7
SAXS analysis	13
XRD analysis	1
Conclusions.....	2
Acknowledgements	3
References.....	3

Introduction

Alginates are linear water-soluble polysaccharides comprising (1-4)-linked units of α -D-mannuronate (M) and β -L-guluronate (G) at different proportions and different distributions in the chain [1, 2].

They are present in brown algae and can also be found in metabolic products of some bacteria [3]. The chemical composition and sequence of the M and G residues depend on the biological source and the state of maturation of the plant [4]. The alginates, as well as all the polysaccharides, are polydisperse in terms of molecular mass so that they are more similar to the synthetic polymers than to other biopolymers such as proteins and nucleic acids [5, 6].

Alginates are well-known natural ionic polysaccharides used mainly as food additives, thickeners, gelling agents, and in the controlled delivery of drugs [7, 8, 9].

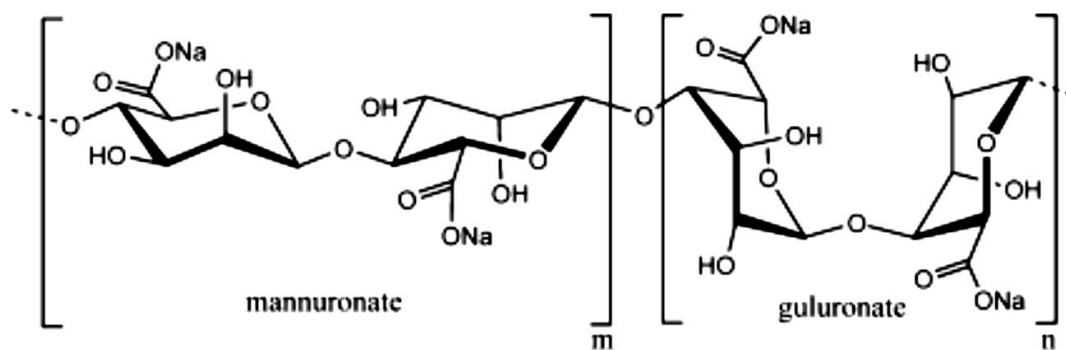


Fig. 1. Representation of the structure of sodium alginate [10].

A magnetic colloid, also known as a ferrofluid (FF), is a colloidal suspension of single-domain magnetic particles, with typical dimensions of about 10 nm, dispersed in a liquid carrier [11].

In order to avoid agglomeration, the magnetic particles have to be coated with a shell of an appropriate material. According to the coating, the FF's are classified into two main groups: surfacted (SFF), if the coating is a surfactant molecule, and bionic (IFF), if it is an electric shell [11, 12].

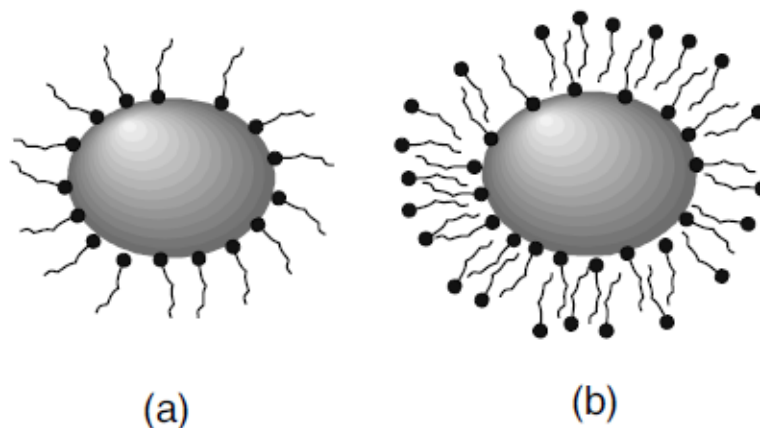


Fig. 2: Sketch of surfacted ferrofluid grains: a) single-layered grains; b) double-layered grains [11]

Cobalt ferrite nanoparticles (CoFe_2O_4) have received increasing attention due to combination of their bulk magnetic properties with the magnetic properties typical of nanoparticles (superparamagnetism) that make them ideal materials for technological and medical applications [14].

By combining the polymer with the nanoparticles, in different forms, can benefit from the combination of features inherent to both the components: magnetic particles and polymer. And, by doing this, the new material obtained can have a wide range of applications.

Experimental section

Materials and membrane preparation

For this study we used alginic acid sodium salt with low viscosity and CoFe_2O_4 nanoparticles.

Alginic sodium salt was purchased from “Alpha Aesar, A Johnson Matthey Company”, it has the viscosity of 40–90 mPas (1% solution) and the pH of 5.0–7.5 (1% solution).

The ferrofluid was prepared at the Institute of Technical Chemistry (Perm) by the coprecipitation of $\text{Fe}(\text{OH})_3$ and $\text{Co}(\text{OH})_2$, ferritisation of hydroxide mixture in 1M alkali aqueous solution, adsorption of lauric acid on ferrite particles and peptisation of hydrophobic precipitate in aqueous solution with sodium n-dodecyl sulphate [14].

The membranes were prepared by casting from aqueous solutions using the method described by Russo [15]. Two solutions of 1% (wt/v) of sodium alginate were prepared, while stirring, at the room temperature for 24h. After a clear solution was obtained, we added 1 mL of CoFe_2O_4 /lauric acid/DDS -Na/ H_2O ferrofluid in one of the solutions and sonicated it to ensure homogeneous distribution of the nanoparticles in the solution.

The solutions were poured, avoiding bubble formation, into a glass Petri dish and kept in an oven, at 50°C , to ensure the evaporation of the solvent. After the solvent was evaporated, the membranes were peeled off and kept in a desiccator till use.

The cross-linking was made with a 3% CaCl_2 solution in which the membranes were immersed for 30 minutes, after that they were dried.

Depending on the technique used, sample preparation might be different and it was presented in the Method section.

Methods of characterization

Small-angle X-ray scattering (SAXS)

Small-angle X-ray scattering (SAXS) is a small-angle scattering (SAS) technique where the elastic scattering of X-rays by a sample which has inhomogeneities in the nanometer range, is recorded at very low angles (typically 0.1 – 10°). This angular range contains information about the shape and size of macromolecules, characteristic distances of partially ordered materials, pore sizes, and other data. SAXS is capable of delivering structural information of macromolecules between 5 and 25 nm, of repeat distances in partially ordered systems of up to 150 nm [16].

X-ray scattering techniques are a family of non-destructive analytical techniques which reveal information about the crystallographic structure, chemical composition, and physical properties of materials and thin films [17].

The small-angle x-ray scattering (SAXS) technique has been applied to investigate membrane structure of alginate in the absence and presence of divalent cation, Ca(II), and CoFe₂O₄ nanoparticles.

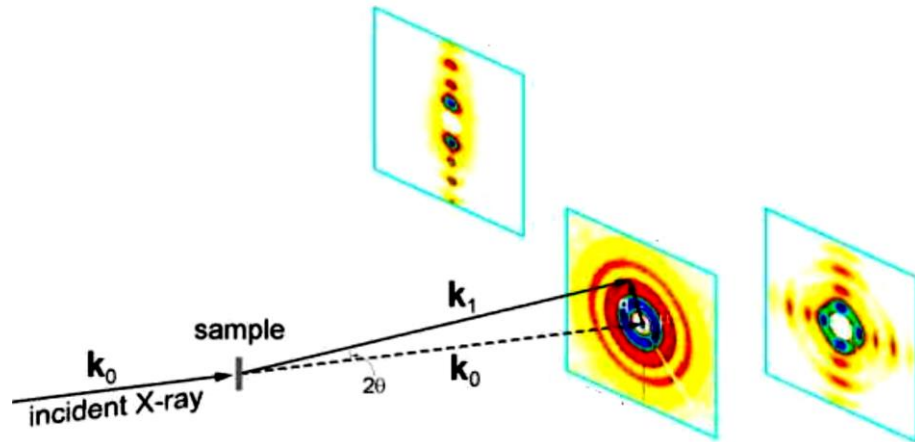


Fig.3. Principle of SAXS [18]

- **Sample preparation**

The SAXS measurements were taken with a Rigaku Small angle X-ray scattering (SAXS) pinhole camera system (Japan) installed with a Rigaku MicroMax-007 HF X-ray source.

The membranes were cut in ~ 1 cm x 1 cm samples and fixed on a one-sided tape. After that, they were mounted on the sample holder facing the beam directly. For the precision of measurement SAXS analysis was made also for the tape without sample.

Atomic Force Microscopy (AFM)

Atomic force microscopy (AFM), also known as scanning-force microscopy (SFM), is a type of scanning probe microscope technique. It works by running a sharp tip attached to a cantilever and sensor over the surface of a sample and measuring the surface forces between the probe and the sample [19]. As the cantilever runs along the sample surface, it moves up and down due to the surface features and the cantilever deflects accordingly. This deflection is usually quantified using an optical sensor, with the laser beam being reflected on the back of the cantilever onto the light detector [19]. AFM does not need to operate in a vacuum and can operate in ambient air or under liquid; hence it is increasingly being used to image biological samples as well as nanoparticles [20, 21, 22].

Atomic force microscopy is a relatively nondestructive technique as compared to conventional scanning electron microscopy and transmission electron microscopy. It also has an additional advantage of 3-dimensional measurements of the surface structure of polymers [23].

The direct visualization of 3-dimensional images of the polymer surfaces is helpful for understanding the effects of changes in processing conditions. The field of nanocomposite is emerging at a rapid rate. Atomic force microscopy can be useful for the characterization of these nanocomposite materials.

The conventional surface characterization techniques provide only pictorial images of the polymer surface [24]. Atomic force microscopy can be exploited to measure the mechanical properties, adhesion forces and structure of the polymer surface by making slight changes in the instrumentation involved. The capability of

AFM to delineate the phase transitions of polymers provides us with important insight regarding the factors that are responsible for the peculiar properties exhibited by polymers. Thus, complete characterization of a polymer surface is possible by atomic force microscopy [25].

- **Sample Preparation**

Atomic force microscopy NTEGRA PRIMA was provided by the company NT-MDT Spectrum Instruments (Zelenograd, Russia). AFM images were recorded at semi-contact mode, *known as tapping mode*, with a standard NSG01 and NSG01_Au tips of 10 nm curvature radius (NT-MDT Spectrum Instruments, Zelenograd, Russia) at room temperature. The imaging rate was 0.3 Hz. Both height image and phase image were recorded.

AFM imaging was performed on films prepared from alginate solution and alginate solution doped with CoFe_2O_4 nanoparticles. Samples were cast as films for ease of imaging. One drop of alginate solution at a given concentration was deposited onto a quartz glass slide, after which the drop was aspirated using a Pasteur pipette and let to dry at room temperature. Calcium chloride at a given concentration was added to the film in a drop-wise fashion to induce cross-linking.

Scanning Electron Microscopy (SEM)

Scanning electron microscopy (SEM) is useful for detailed study of a specimen's surface. A high-energy electron beam scans across the surface of a specimen, usually coated with a thin film of gold or platinum to improve contrast and the signal-to-noise ratio [26].

As the beam scans across the sample's surface, interactions between the sample and the electron beam result in different types of electron signals emitted at or near the specimen surface [23, 24].

These electronic signals are collected, processed, and eventually translated as pixels on a monitor to form an image of the specimen's surface topography that appears three dimensional [29].

- **Sample preparation**

The surface of the samples used in this study were analyzed by a Hitachi SU8020 (Japan) scanning electron microscope at an accelerated voltage of 2 kV. Prior to observation, the samples were coated with a thin layer of gold under a vacuum.

X-ray Diffraction (XRD)

X-ray diffraction (XRD) is one of the most important non-destructive tools to analyze all kinds of matter. The technique is used for the identification of crystalline phases of various materials and the quantitative phase analysis subsequent to the identification [30].

X-ray diffraction techniques are superior in elucidating the three-dimensional atomic structure of crystalline solids. The properties and functions of materials largely depend on the crystal structures. X-ray diffraction techniques have, therefore, been widely used as an indispensable means in materials research, development and production [31].

- **Sample preparation**

The presence of the CoFe_2O_4 nanoparticles in the membrane was characterized by the XRD technique using X-ray diffractometer (PANalytical Empryan) with $\text{Cu K}\alpha$ radiation ($\lambda = 0.15406$ nm) in a wide range of 2θ ($5^\circ < 2\theta < 80^\circ$).

The samples were prepared in a similar manner as the ones from Atomic Force Microscopy. Instead of using quartz glass slide, the sample was casted on a zero diffraction plate made of silicon cut at special orientation.

Results and Discussion

Surface morphology

As previously stated, AFM was chosen for imaging as it is an imaging method that provides nanometer resolution and three-dimensional surface imaging, requires minimal sample preparation and allows imaging in ambient and liquid conditions.

In Figure 4, can be seen from the surface imaging that the addition of CoFe_2O_4 nanoparticles increase the inhomogeneity on the surface of the membranes and aggregates of alginate tend to form.

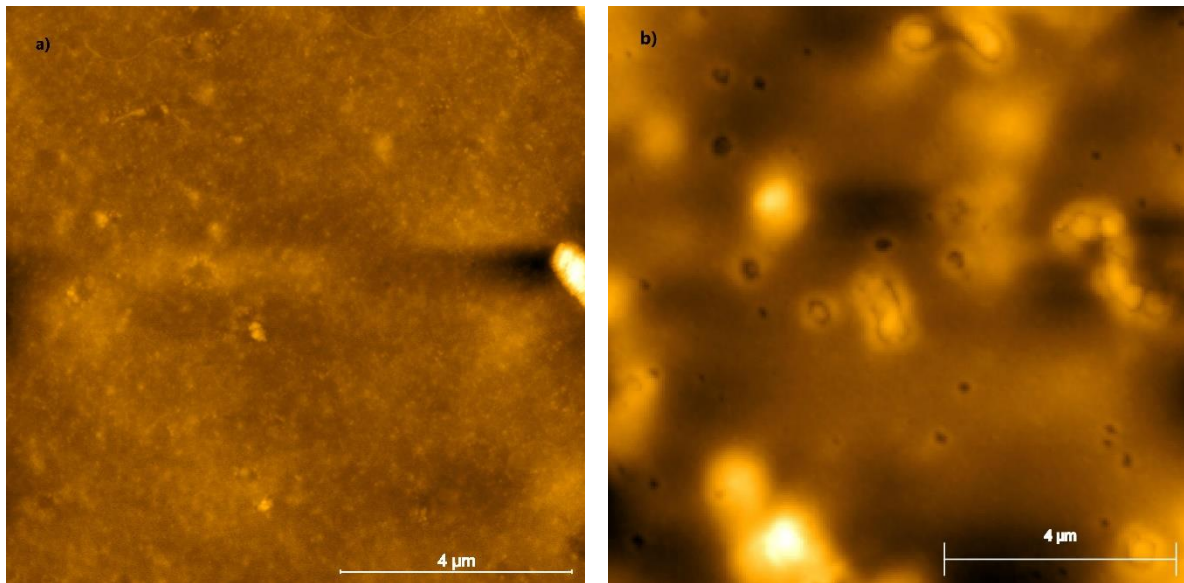
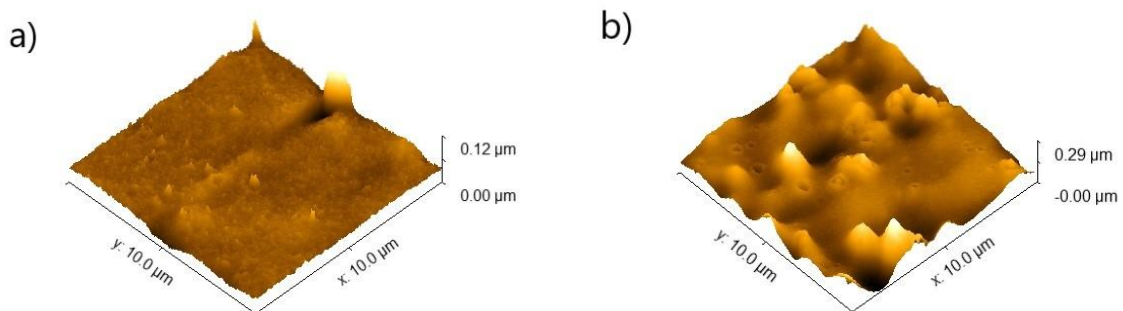


Fig. 4. AFM images of alginate membranes at 10 μm : a) 1% sodium alginate and b) 1% alginate with CoFe_2O_4 nanoparticles

Based on the roughness parameters of 1% alginate membrane ($S_q = 5,74 \text{ nm}$ and $S_a = 3,41 \text{ nm}$) and 1% alginate membrane with nanoparticles ($S_q = 44,58 \text{ nm}$ and $S_a = 32,09 \text{ nm}$), with AFM imaging at a higher resolution, can be observed that by adding the nanoparticles the surface roughness increases and bigger pores appear on the surface. The pore size observed on the membrane with nanoparticles had an average of 30 nm. In figure 5 are presented the 3D AFM images at a higher resolution in which the pores can be observed.



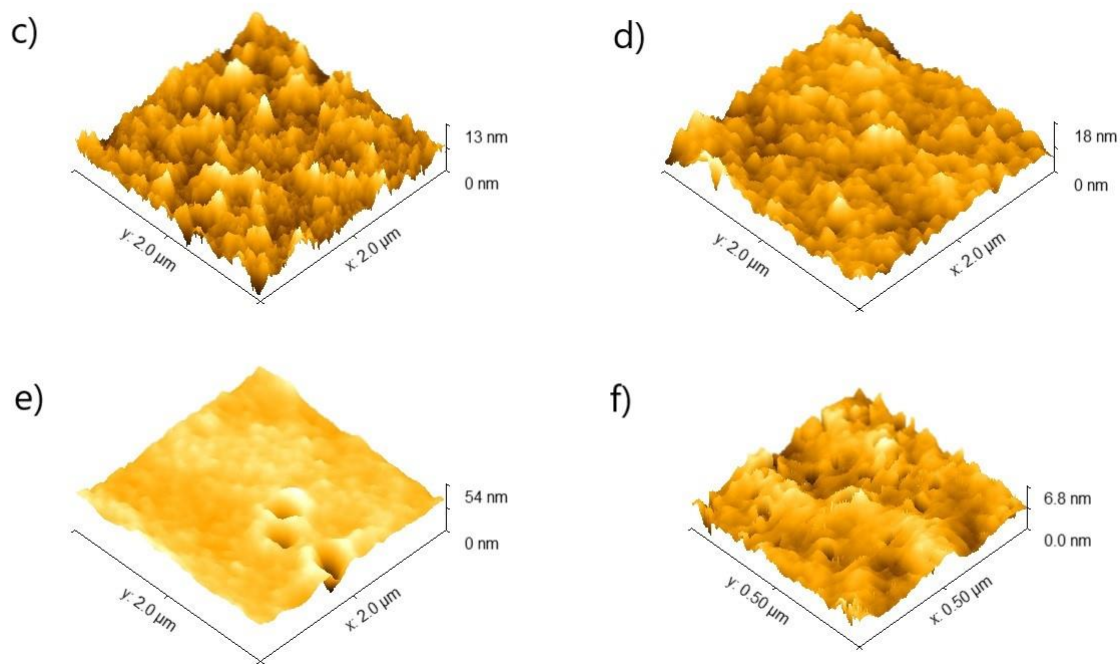


Fig. 5. AFM 3D view of the membranes surface:

- a) 1% alginate membrane (Scanning area = $10 \mu\text{m}^2$)
- b) 1% alginate membrane with nanoparticles (Scanning area = $10 \mu\text{m}^2$)
- c) 1% alginate membrane (Scanning area = $2 \mu\text{m}^2$)
- d) 1% alginate membrane with nanoparticles (Scanning area = $2 \mu\text{m}^2$)
- e) 1% alginate membrane with nanoparticles and visible pores (Scanning area = $2 \mu\text{m}^2$)
- f) 1% alginate membrane with nanoparticles (Scanning area = $0,5 \mu\text{m}^2$)

The data obtained from SEM is in accordance with the observation made from AFM imaging.

It can be seen in the SEM images of the 1% alginate membrane, without and with nanoparticles, that the surface changes morphology (Figure 6 a) and b)). By adding nanoparticles, on the surface of the membrane aggregates with a mean diameter of 50 nm are formed and there can be observed that the nanoparticles are heterogeneous spread on the surface in “pond” like formations.

The aggregates observed in figure 6b could be caused by the cross-linking effect of the divalent and trivalent cations present in the nanoparticles formulation (Co^{2+} and Fe^{3+}). It is known that divalent and trivalent cations cross-link the polymeric chains of alginate and rearrange their structure according to the egg-box model (Figure 7).

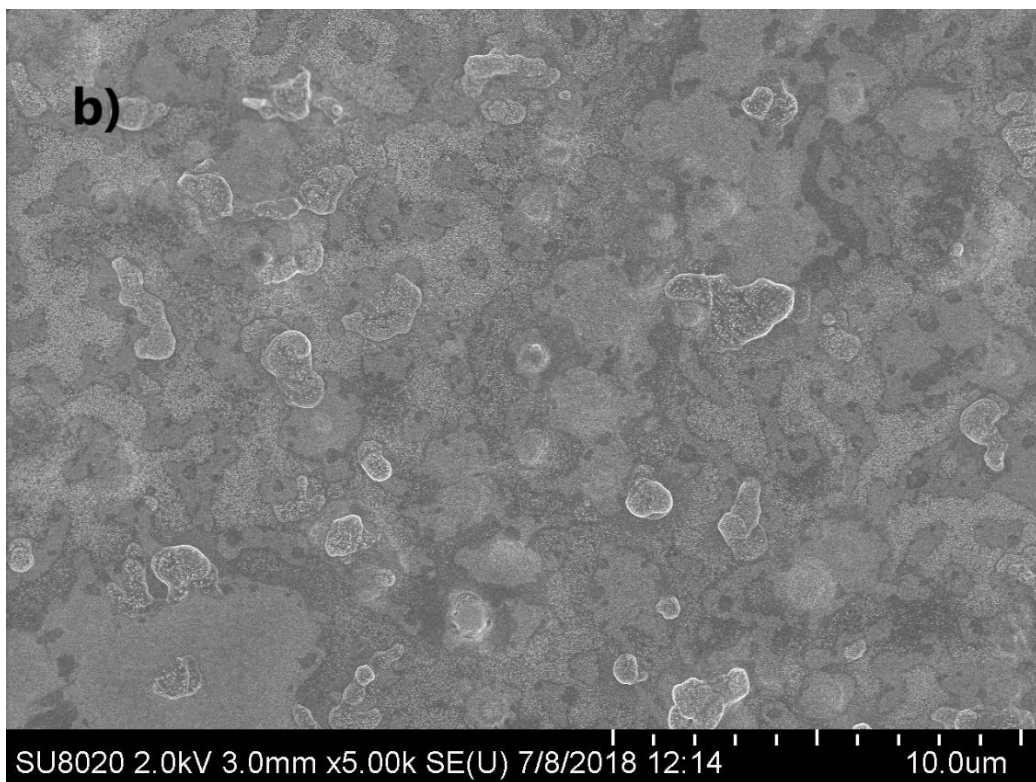
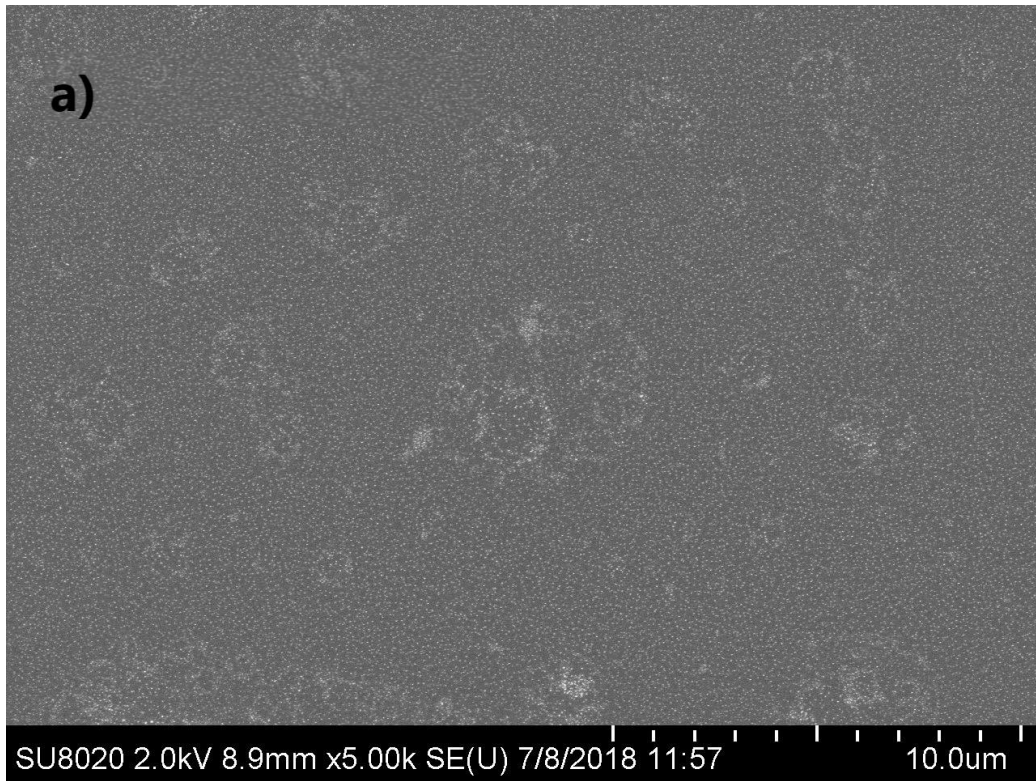


Fig. 6. SEM images of the surface of membranes : a) 1% alginate membrane
b) 1% alginate membrane with nanoparticles

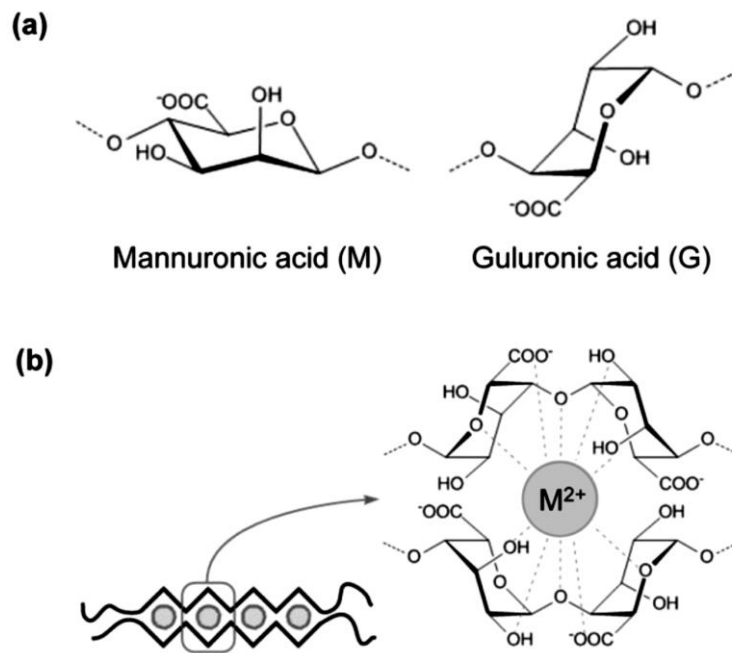


Fig. 7. a) Structure of the alginate monomers: D-mannuronic acid (left) and L-guluronic acid (right). **b)** Egg-box structure of the cross-linking between a divalent cation and G monomers of two different alginate chains [32]

The effect of cross-linking with Ca^{2+} ions can be seen in the high images from AFM (Figure 8) and the SEM images (Figure 10).

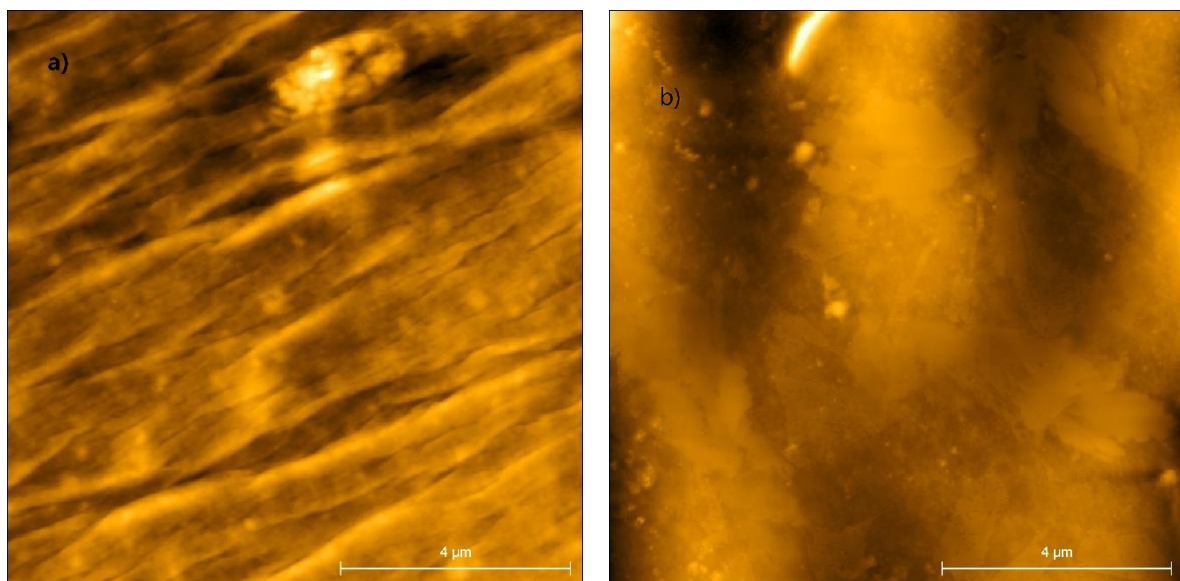


Fig. 8. AFM high image of a) 1% sodium alginate membrane cross-linked with Ca^{2+} b) 1% sodium alginate membrane and nanoparticles cross-linked with Ca^{2+}

From the AFM image of the sodium alginate membrane cross-linked with Ca^{2+} ions (Figure 8a) can be observed a layered arrangement of the polymer, which isn't found at the cross-linked membranes that has nanoparticles. Also, the roughness parameters of the cross-linked membrane increased ($S_q = 29,55 \text{ nm}$ and $S_a = 22,55 \text{ nm}$) and for the membrane with nanoparticles decreased ($S_q = 27,46 \text{ nm}$ and $21,66 \text{ nm}$).

In the case of divalent cations, egg box model has illustrated that the cations bond with the blocks of alginate polymers in a planar two-dimensional manner, and the extent of binding increases with an increasing of ionic radius. On the other hand, trivalent cations are expected to form a three dimensional valent bonding structure with the alginate [33].

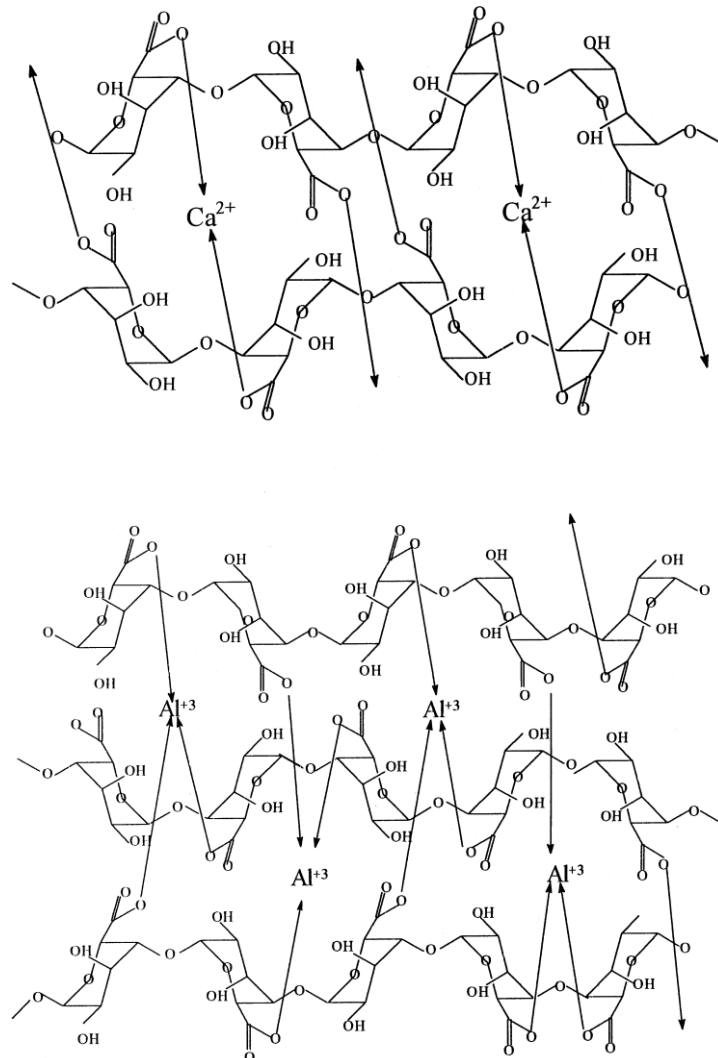


Fig. 9. Example of the mechanism of reaction between calcium and aluminum cations and sodium alginate matrices [33].

The cross-linking process is known to be influenced by the ionic radius of the cation. Cations with larger ion radius ($\text{Fe}^{3+} = 1.35 \text{ \AA}$) can form a tighter structure compared with cations with smaller ion radius ($\text{Ca}^{2+} = 1.0 \text{ \AA}$) because cations they are expected to fill a larger space between the blocks of alginate polymers, resulting a tighter arrangement of cross-linked alginate polymers.

Compared with divalent cations, the binding extent of trivalent cations with alginate is enhanced. Trivalent cations could interact with three carboxylic groups of different alginate chains at the same time, lead to a larger coordination number ($(\text{COO})_3\text{M}$) and form a three-dimensional valent bonding structure, resulting in a more compact network. These effects were reported in several papers from Al- Musa [33], Yang [34] and Winkleman [35].

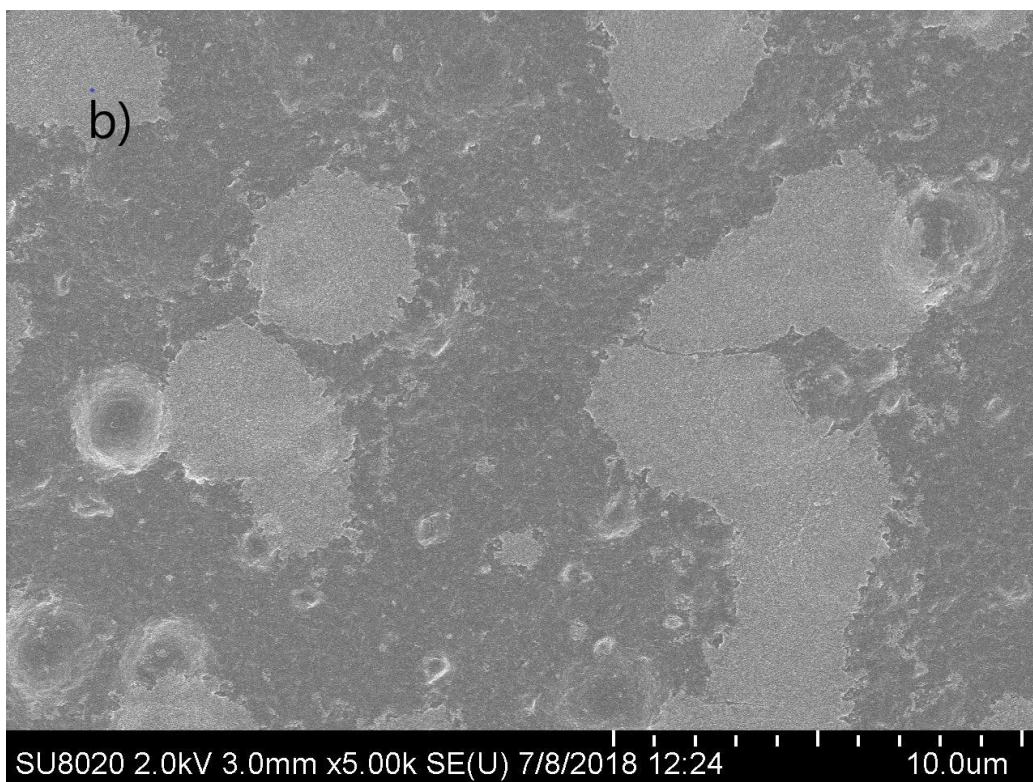
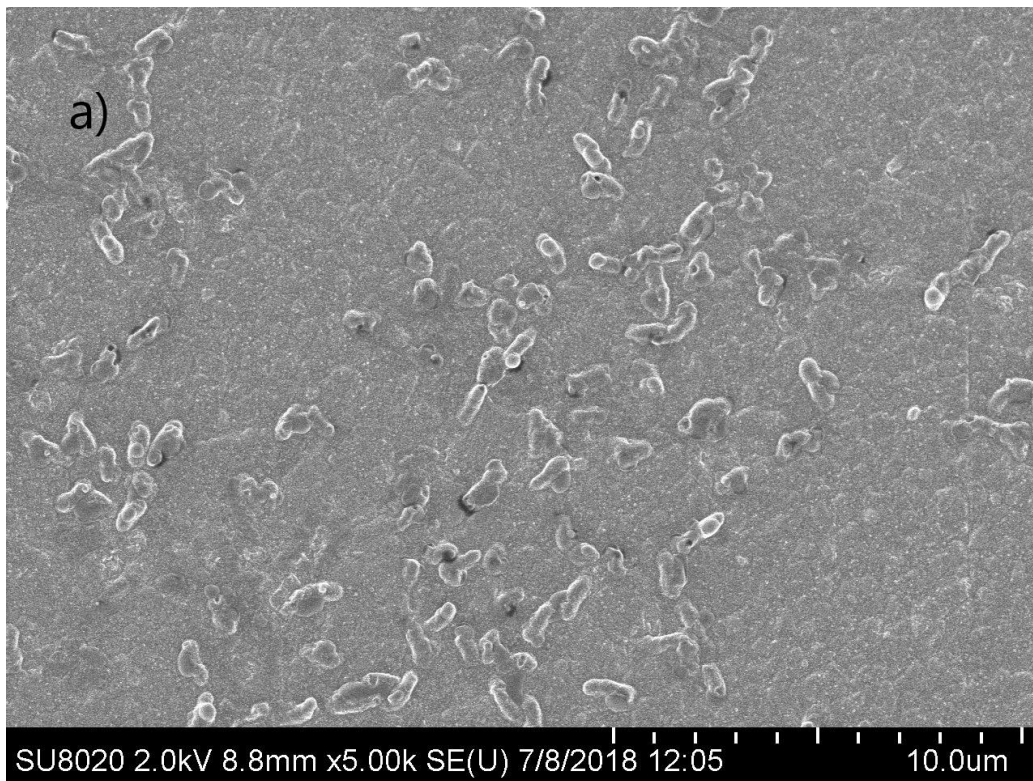
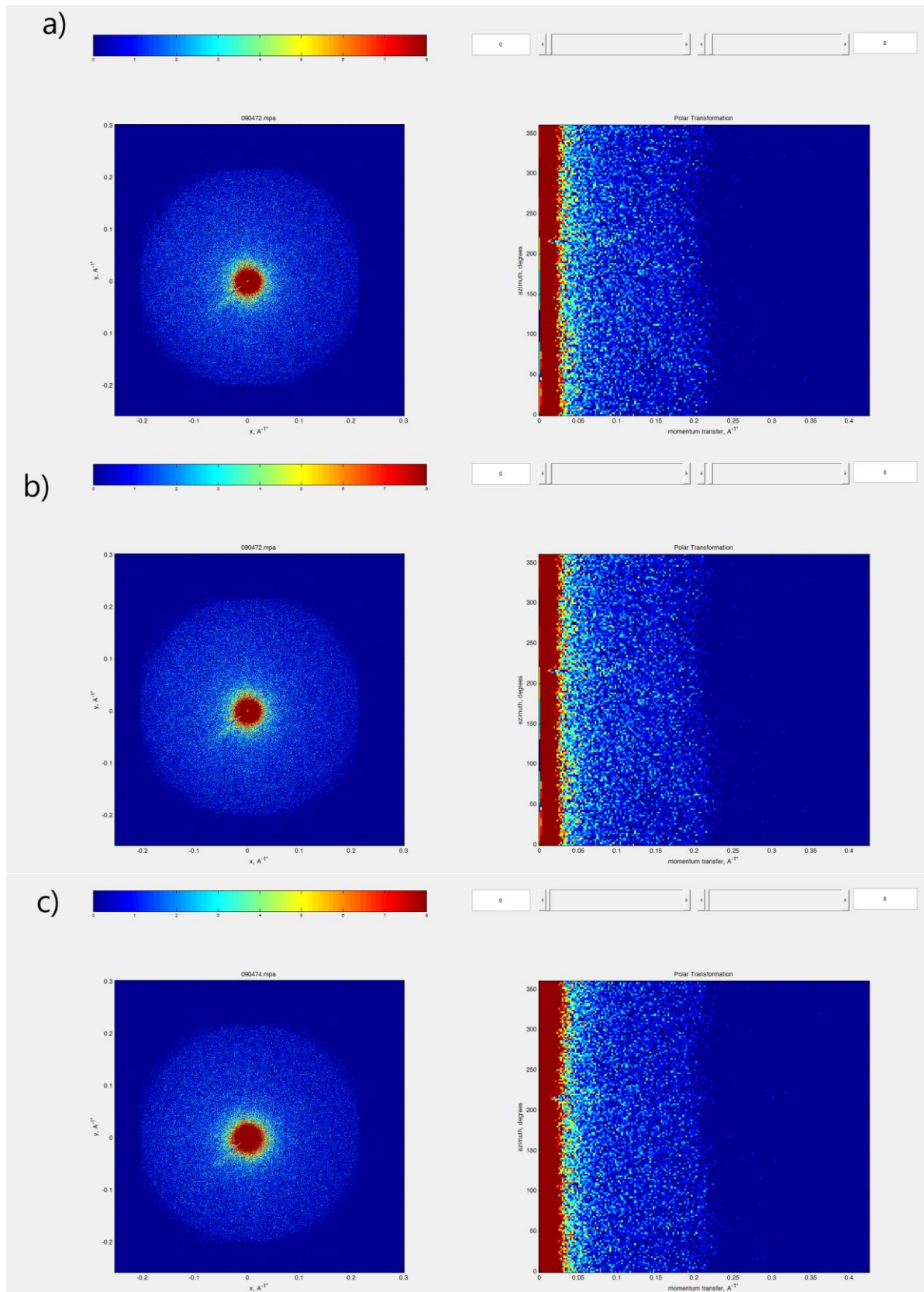


Fig. 10. SEM image of the cross-linked membranes with Ca^{2+} : a) without nanoparticles and b) with nanoparticles

As can be seen, the presence of Fe^{3+} and Co^{2+} in the formulation of the cross-linked membranes compete with the effect of Ca^{2+} cations and the surface from figure 10b looks smoother than the one from figure 10a.

SAXS analysis

The scattering patterns obtained from the SAXS analysis are presented in figure 11 a-e.



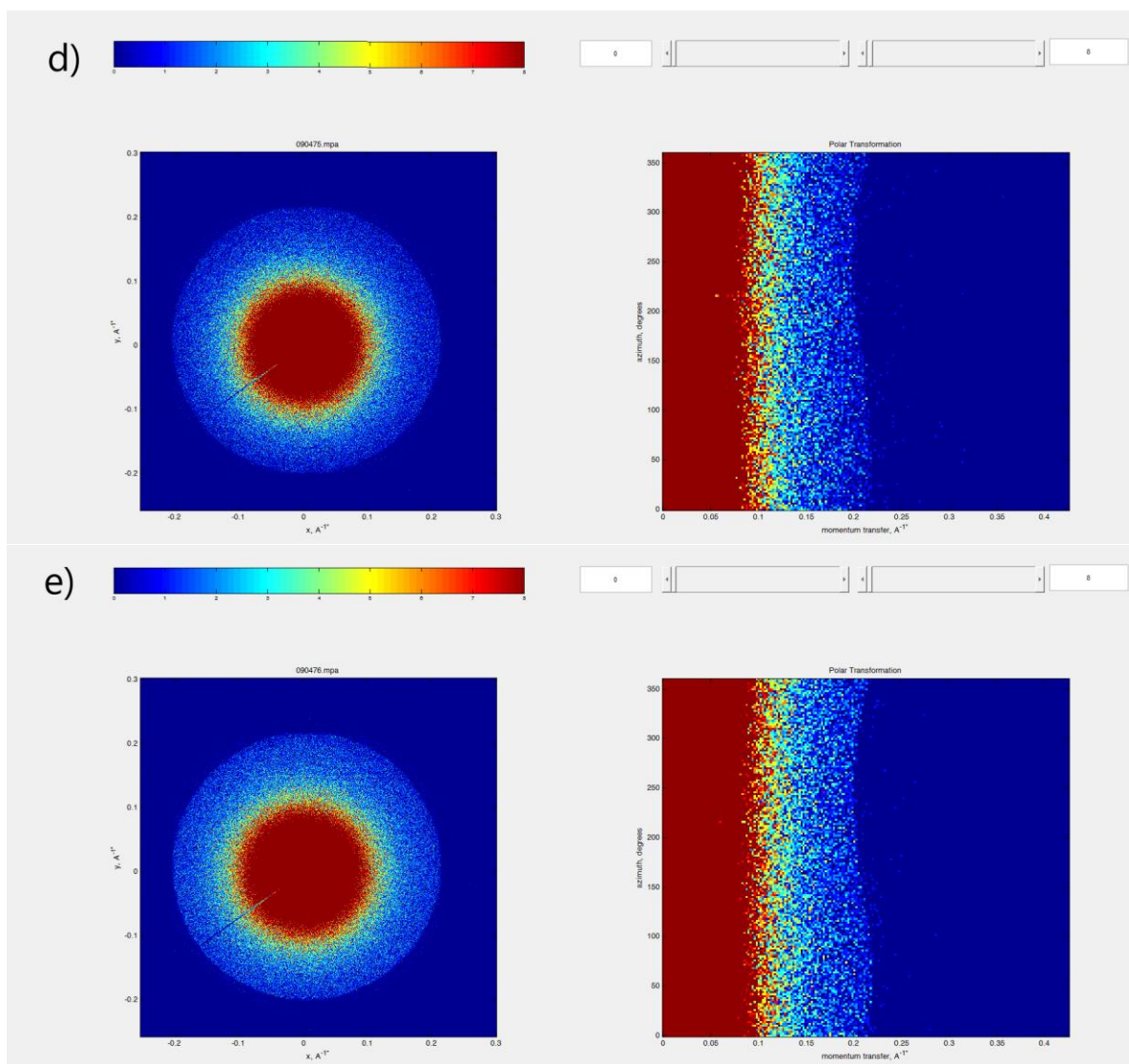


Fig. 11. Scattering patterns of: a) one-sided tape; b) 1% sodium alginate membrane; c) 1% sodium alginate membrane cross-linked with Ca^{2+} ; d) 1% sodium alginate membrane and nanoparticles; e) 1% sodium alginate membrane and nanoparticles cross-linked with Ca^{2+}

From the data obtained, the scattering that occurred from the one-sided tape was subtracted and the SAXS data was transformed from 2D to 1D, following curves being obtained (figure 12). The curves were analyzed using Fitter, a program developed by LIT and FLNF (YuMO group), JINR, Dubna.

The fitting models were analysed on different Q (Å^{-1}) intervals and the models identified are presented in Table 1.

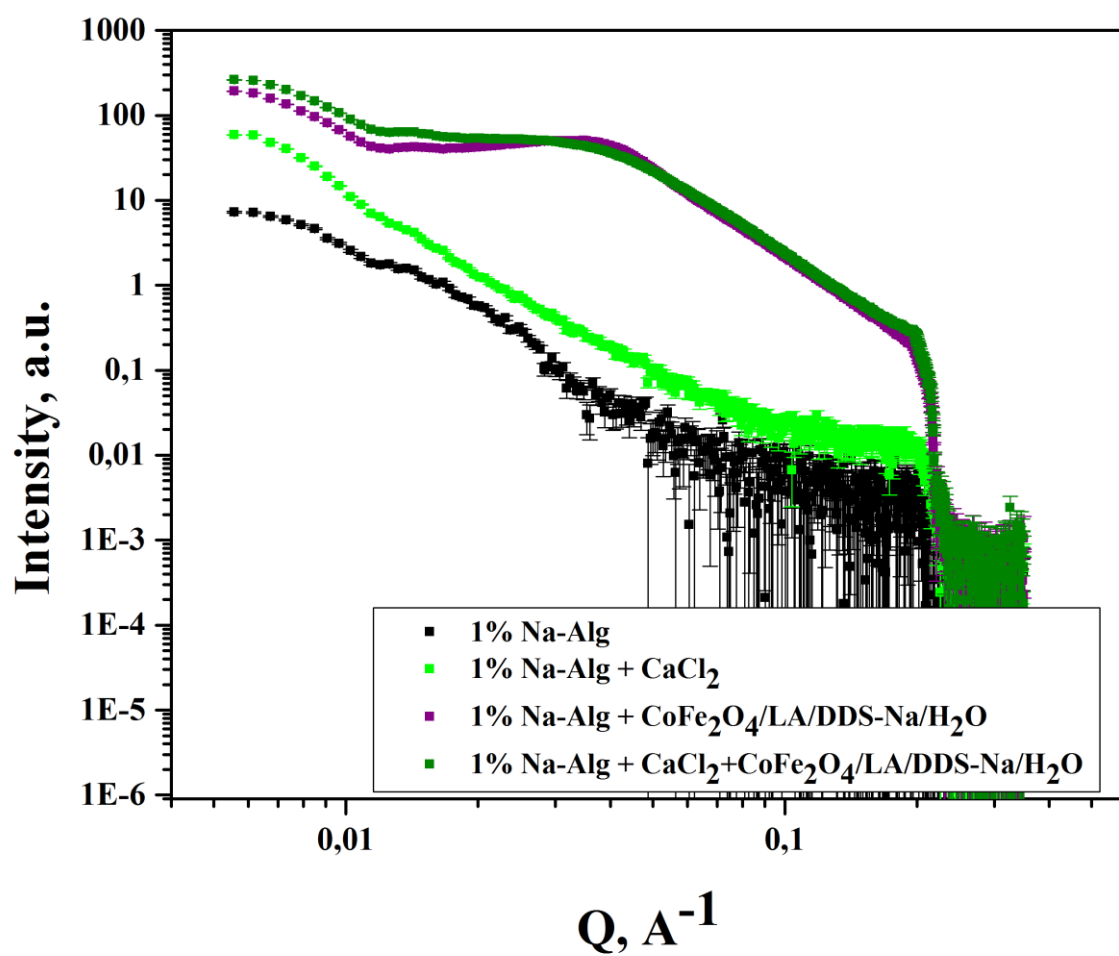


Fig. 12. SAXS curves of the alginate membranes

Table 1. Models and scattering parameters obtained from SAXS data using Fitter program

Sample	Q-domain	Model	Scatterer Object Parameters
1% Na-Alg	0.045÷0.11	Ball	Radius=5306.2 A
	0.04÷0.25	Biaxial ellipsoid	Axis=865.7 A Excentricity=0.9
1% Na-Alg + CaCl ₂	0.0044÷0.023	Parallelepiped	A=7306.8 A B= 7928.1 A C= 7956.3 A
	0.03÷0.05	Biaxial ellipsoid	Axis= 0.5927 A Excentricity= 5078
	0.05÷0.1	Triaxial ellipsoid	a= 2092.2 A b=6351.5 A c= 1065.9 A
	0.1÷0.18	Biaxial ellipsoid	Axis=30.8 A Excentricity=9631
	0.18÷0.24	Biaxial ellipsoid	Axis=62.7 A Excentricity=9647
1% Na-Alg nanoparticles +	0.0045÷0.0115	Ball	Radius=5298.3 A
	0.0115÷0.023	Triaxial ellipsoidal coreshell	Semiasis a of core=869.5 A Semiasis b of core=19.85 A Semiasis c of core=18.5 A Thickness of shell=6500.3 A
	0.02÷0.037	Triaxial ellipsoidal coreshell	Semiasis a of core=152.5 A Semiasis b of core=138.7 A Semiasis c of core=137.8 A Thickness of shell=6903.5 A
	0.038÷0.084	Ball	Radius=5344.3 A
1% Na-Alg nanoparticles +CaCl ₂	0.006÷0.0115	Biaxial ellipsoid	Axis=191.5A Excentricity=220
	0.0115÷0.03	Ball	Radius=5414.0 A
	0.04÷0.095	Biaxial ellipsoid	Axis=563.3A Excentricity=352

XRD analysis

Fig. 13 shows the XRD patterns of neat alginate powder, 1% sodium alginate membrane and cross-linked membrane with Ca^{2+} cations. Alginate powder exhibited two broad peaks with central positions at $2\theta = 15,7^\circ$ and $24,9^\circ$, respectively, which indicate two different amorphous regions. But these two broad peaks do not correlate with the data reported in literature [36, 37, 38], where is stated that alginate exhibits two broad peaks with central positions at $2\theta = 13^\circ$ and 21° .

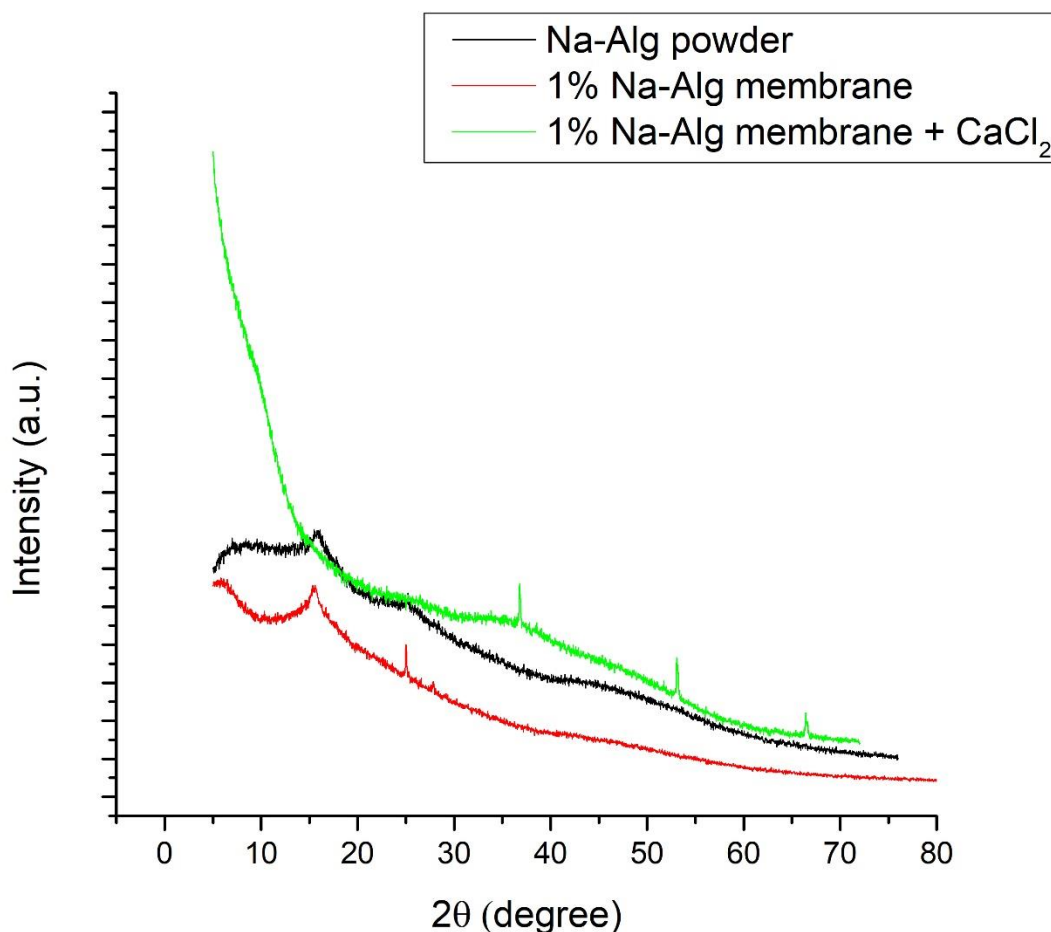


Fig. 13. XRD patterns of neat alginate powder, 1% sodium alginate membrane and cross-linked membrane with Ca^{2+} cations

It can be noticed that for the alginate film, the peak at $24,9^\circ$ is sharper than for the neat alginate powder due to the likely rearrangement of the alginate chains. Such phenomenon was also observed in plasticized chitosan samples obtained by thermo-mechanical mixing [36, 39], and could be a influence of the preparation method, taking into consideration that the membranes were dried at 50°C . This procedure could have influenced the microstructure of the membranes and there are studies in literature which state that the procedure of drying the membranes can influence the final structure of the product [40, 41, 42], so further investigations are required.

In the XRD spectra of uncross-linked and cross-linked alginate membrane the characteristic peaks disappear, and this could indicate that Na^+ cations are replaced by the Ca^{2+} cations.

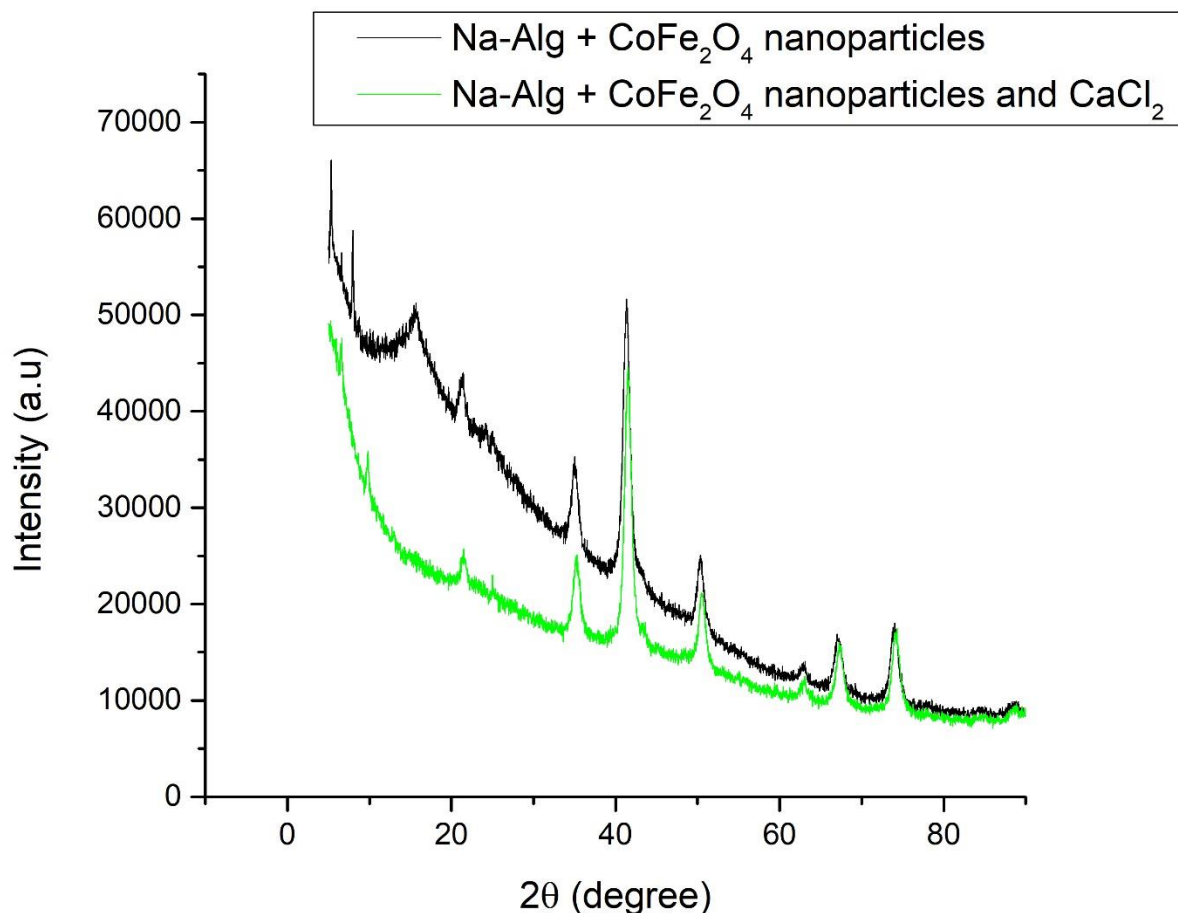


Fig. 14. XRD patterns of 1% sodium alginate membranes with CoFe_2O_4 nanoparticles and cross-linked with Ca^{2+} cations

The patterns of both samples show prominent peaks belonging to the cubic spinel type lattice of CoFe_2O_4 , which matches well with the standard XRD pattern (JCPDS Card No: 22-1086) and the characteristic peaks from the polymer matrix can be observed.

Conclusions

The surface morphology of uncross-linked and cross-linked alginate membranes containing CoFe_2O_4 nanoparticles was investigated through the use of AFM and SEM and the XRD analysis confirm the CoFe_2O_4 nanoparticles presence in the membranes.

AFM experiments performed on alginate membrane containing nanoparticles showed a rough surface and the fact that the presence of nanoparticles promote the formation of pores.

The presence of Fe^{3+} and Co^{2+} cations in the formulation of the cross-linked membranes compete with the effect of Ca^{2+} cations on the alginate polymer, as can be seen in the AFM and SEM pictures.

Further structural investigations are required to have a better understanding on the factors that can influence the structure of alginate membranes.

Comparing the two-dimensional data obtained from AFM and SEM with the data obtained from the SAXS analysis, we can conclude that the SAXS analysis allowed us to have volume information about the structures present in the membranes:

- a) in the SEM image of 1% sodium alginate membrane (figure 6a) there can be identified the ball and ellipsoidal structures
- b) SAXS allowed us to confirm the observations made about the SEM images (figure 6b and figures 7a and b) related to the effect of nanoparticles and the cross-linking process with Ca^{2+} cations of the membranes by revealing the complex structures formed, which correspond dimensional with the ones that appear on the surface of the membranes;
- c) the structures identified by SAXS data can be related to the information from literature regarding the effect of divalent and trivalent cation.

Acknowledgements

I would like to express my gratitude to my scientific supervisor Dr. Maria Bălăşoiu for the opportunity to work with her and for all the help that she gave me during my stay in Dubna. Thanks goes to Dr. Yulia Gorshkova, Dr. Vitaly Turchenko, Dr. Alexander Kuklin, Dr. Nikolai Lizunov and Dr. Vadim Skoy for their support and expertise given during my research.

I would also like to thank the organizers of Summer Student Program for providing education opportunities and valuable experiences. Thanks to Mrs. Elena Karpova and Mrs. Elizaveta Tsukanova for their assistance in solving all the issues and to JINR for the financial support.

Special thanks to my dear professor Assoc. Prof. Vlad Chiriac for the support given and for persuading me to apply for the program and also to my university who made it possible for me to participate in SSP this summer.

References

- [1] H. Grasdalen, B. Larsen, and O. Smisrod, " ^{13}C -n.m.r. studies of monomeric composition and sequence in alginate," *Carbohydr. Res.*, vol. 89, no. 2, pp. 179–191, 1981.
- [2] J. Wingender, T. R. Neu, and H.-C. Flemming, *Microbial Extracellular Polymeric Substances: Characterization, Structure and Function*. Springer, 1999.
- [3] W. Mushollaeni and E. R. S, "Optimizing the Use of Alginate from Sargassum and Padina as Natural Emulsifier and Stabilizer in Cake," *J. Agric. Food Technol.*, vol. 2, no. 7, pp. 108–112, 2012.
- [4] H. H. Tønnesen and J. Karlsen, "Alginate in drug delivery systems," *Drug Dev. Ind. Pharm.*, vol. 28, no. 6, pp. 621–630, 2002.
- [5] M. Rinaudo, "Biomaterials based on a natural polysaccharide: alginate," *Rev. Espec. en Ciencias Químico-Biológicas*, vol. 17, no. 1, pp. 92–96, 2014.
- [6] M. J. Gidley and J. S. G. Reid, *Galactomannans and other cell wall storage polysaccharides in seeds*. Taylor & Francis Group, 2006.
- [7] W. R. Gombotz and S. Wee, "Protein release from alginate matrixes," *Adv. Drug Deliv. Rev.*, vol. 31, no. 3, pp. 267–285, 1998.
- [8] Ø. Holte, E. Onsøyen, R. Myrvold, and J. Karlsen, "Sustained release of water-

- soluble drug from directly compressed alginate tablets," *Eur. J. Pharm. Sci.*, vol. 20, no. 4–5, pp. 403–407, 2003.
- [9] H. Liang-Nian, R. Robin D., S. Dangsheng, T. Pietro, and Z. Conrad, *Soil Degradable Bioplastics for a Sustainable Modern Agriculture*. Springer US, 2017.
- [10] O. Philippova, A. Barabanova, V. Molchanov, and A. Khokhlov, "Magnetic polymer beads: Recent trends and developments in synthetic design and applications," *Eur. Polym. J.*, vol. 47, no. 4, pp. 542–559, 2011.
- [11] K. Raj and R. J. Boulton, "Ferofluids - Properties and applications," *Mater. Des.*, vol. 8, no. 4, pp. 233–236, 1987.
- [12] H. Shokrollahi, "Structure, synthetic methods, magnetic properties and biomedical applications of ferofluids.," *Mater. Sci. Eng. C. Mater. Biol. Appl.*, vol. 33, no. 5, pp. 2476–2487, 2013.
- [13] J. Roger, J. N. Pons, R. Massart, A. Halbreich, and J. C. Bacri, "Some biomedical applications of ferofluids," *Eur. Phys. J. Appl. Phys.*, vol. 5, no. 3, pp. 321–325, 1999.
- [14] M. Balasoïu *et al.*, "Microstructure investigation of a CoFe₂O₄/lauric acid/DDS-Na/H₂O ferofluid," *J. Oproelectronics Adv. Mater.*, vol. 17, no. 7–8, pp. 1114–1121, 2015.
- [15] R. Russo, M. Malinconico, and G. Santagata, "Effect of cross-linking with calcium ions on the physical properties of alginate films," *Biomacromolecules*, vol. 8, no. 10, pp. 3193–3197, 2007.
- [16] O. Glatter and O. Kratky, "Small Angle X-ray Scattering," *Academic Press Inc. (London) LTD*. p. 262, 1982.
- [17] G. Gebel and O. Diat, "Neutron and X-ray scattering: Suitable tools for studying ionomer membranes," *Fuel Cells*, vol. 5, no. 2, pp. 261–276, 2005.
- [18] M. Fujimura, T. Hashimoto, and H. Hawaii, "Small-Angle X-ray Scattering Study of Perfluorinated Ionomer Membranes. 1. Origin of Two Scattering Maxima," *Macromolecules*, vol. 14, no. 5, pp. 1309–1315, 1981.
- [19] J. Sitterberg, A. Özçetin, C. Ehrhardt, and U. Bakowsky, "Utilising atomic force microscopy for the characterisation of nanoscale drug delivery systems," *Eur. J. Pharm. Biopharm.*, vol. 74, no. 1, pp. 2–13, 2010.
- [20] X. Liang, G. Mao, and K. Y. S. Ng, "Probing small unilamellar EggPC vesicles on mica surface by atomic force microscopy," *Colloids Surfaces B Biointerfaces*, vol. 34, no. 1, pp. 41–51, 2004.
- [21] B. Ruozi, G. Tosi, F. Forni, M. Fresta, and M. A. Vandelli, "Atomic force microscopy and photon correlation spectroscopy: Two techniques for rapid characterization of liposomes," *Eur. J. Pharm. Sci.*, vol. 25, no. 1, pp. 81–89, 2005.
- [22] B. Ruozi *et al.*, "AFM phase imaging of soft-hydrated samples: A versatile tool to complete the chemical-physical study of liposomes," *J. Liposome Res.*, vol. 19, no. 1, pp. 59–67, 2009.
- [23] R. N. Jagtap and A. H. Ambre, "Overview literature on atomic force microscopy (AFM): Basics and its important applications for polymer characterization," *Indian J. Eng. Mater. Sci.*, vol. 13, no. August, pp. 368–384, 2006.
- [24] M. Marrese, V. Guarino, and L. Ambrosio, "Atomic Force Microscopy: A Powerful Tool to Address Scaffold Design in Tissue Engineering," *J. Funct. Biomater.*, vol. 8, no. 1, p. 7, 2017.
- [25] M. Raposo, Q. Ferreira, and P. a Ribeiro, "A Guide for Atomic Force Microscopy Analysis of Soft- Condensed Matter," *Mod. Res. Educ. Top. Microsc.*, pp. 758–

- 769, 2007.
- [26] I. Arzate-Vázquez *et al.*, “Microstructural characterization of chitosan and alginate films by microscopy techniques and texture image analysis,” *Carbohydr. Polym.*, vol. 87, no. 1, pp. 289–299, 2012.
- [27] A. Kowalik klimczak, A. Bednarska, and M. G. R. A. Dkowski, “Scanning Electron Microscopy (Sem) in the Analysis of the Structure,” *Probl. Eksploat. – Maint. Probl.*, pp. 119–128, 2016.
- [28] S. Z. Abdullah, P. R. Bérubé, and D. J. Horne, “SEM imaging of membranes: Importance of sample preparation and imaging parameters,” *J. Memb. Sci.*, vol. 463, pp. 113–125, 2014.
- [29] K. J. Kim, M. R. Dickson, A. G. Fane, and J. D. Fell, “Electron microscopy in synthetic polymer membrane research,” *J. Microsc.*, vol. 162, no. 162, pp. 403–413, 1991.
- [30] N. V Podberezskaya, W. L. Bragg, and S. Division, “X-Ray Diffraction Analysis : a Brief History and Achievements,” *J. Struct. Chem.*, vol. 53, no. S1, pp. 1–3, 2012.
- [31] S. A. Speakman, “Introduction to X-Ray Powder Diffraction Data Analysis,” *Mater. Sci.*, p. 20, 2014.
- [32] S. Pistone, D. Qoragllu, G. Smistad, and M. Hiorth, “Formulation and preparation of stable cross-linked alginate-zinc nanoparticles in the presence of a monovalent salt,” *Soft Matter*, vol. 11, no. 28, pp. 5765–5774, 2015.
- [33] S. Al-Musa, D. Abu Fara, and A. A. Badwan, “Evaluation of parameters involved in preparation and release of drug loaded in crosslinked matrices of alginate,” *J. Control. Release*, vol. 57, no. 3, pp. 223–232, 1999.
- [34] C. H. Yang *et al.*, “Strengthening alginate/polyacrylamide hydrogels using various multivalent cations,” *ACS Appl. Mater. Interfaces*, vol. 5, no. 21, pp. 10418–10422, 2013.
- [35] A. Winkleman, J. P. Bracher, I. Gitlin, and M. G. Whitesides, “Fabrication and Manipulation of Ionotropic Hydrogels Crosslinked by Paramagnetic Ions,” *Chem. Mater.*, vol. 6, no. 8, pp. 1362–1368, 2013.
- [36] C. Gao, E. Pollet, and L. Avérous, “Properties of glycerol-plasticized alginate films obtained by thermo-mechanical mixing,” *Food Hydrocoll.*, vol. 63, pp. 414–420, 2017.
- [37] E. D. T. Atkins, I. A. Nieduszynski, W. Mackie, K. D. Parker, and E. E. Smolko, “Structural components of alginic acid. II. The crystalline structure of poly- α -L-guluronic acid. Results of X-ray diffraction and polarized infrared studies,” *Biopolymers*, vol. 12, no. 8, pp. 1879–1887, 1973.
- [38] E. D. T. Atkins, I. A. Nieduszynski, W. Mackie, K. D. Parker, and E. E. Smolko, “Structural components of alginic acid. I. The crystalline structure of poly- β -D-mannuronic acid. Results of X-ray diffraction and polarized infrared studies,” *Biopolymers*, vol. 12, no. 8, pp. 1865–1878, 1973.
- [39] M. Matet, M. C. Heuzey, E. Pollet, A. Ajjji, and L. Avérous, “Innovative thermoplastic chitosan obtained by thermo-mechanical mixing with polyol plasticizers,” *Carbohydr. Polym.*, vol. 95, no. 1, pp. 241–251, 2013.
- [40] H. Haidara, L. Vonna, and L. Vidal, “Unrevealed self-assembly and crystallization structures of Na-alginate, induced by the drying dynamics of wetting films of the aqueous polymer solution,” *Macromolecules*, vol. 43, no. 5, pp. 2421–2429, 2010.
- [41] L. Feng, Y. Cao, D. Xu, S. Wang, and J. Zhang, “Molecular weight distribution, rheological property and structural changes of sodium alginate induced by

- ultrasound," *Ultrason. Sonochem.*, vol. 34, pp. 609–615, 2017.
- [42] M. Sozo *et al.*, "Heat treatment of calcium alginate films obtained by ultrasonic atomizing: Physicochemical characterization," *Food Hydrocoll.*, vol. 51, pp. 193–199, 2015.